

## DISPLACEMENT-BASED SEISMIC DESIGN OF EXTENDED PILE-SHAFTS FOR BRIDGE STRUCTURES

S. T. Song<sup>1</sup> and Y. H. Chai<sup>2</sup>

<sup>1</sup> Assistant Professor, Dept. of Civil Engineering, University of Louisiana, Lafayette, Louisiana, USA

<sup>2</sup> Professor, Dept. of Civil and Environmental Engineering, University of California, Davis, California, USA  
Email: [ssong@louisiana.edu](mailto:ssong@louisiana.edu), [yhchai@ucdavis.edu](mailto:yhchai@ucdavis.edu)

### ABSTRACT :

Seismic design of extended pile-shafts requires a consideration of the influence of the surrounding soil on the overall response of the soil-pile system. A procedure for seismic design of extended pile-shafts for bridge structures is presented in this paper. The design methodology follows the displacement-based design philosophy, where a target displacement is specified as the basis for design to ensure good performance. The procedure is capable of incorporating soil effects into the design process so that the influence of soil stiffness and strength on the seismic response of the structure can be accounted for. The design procedure involves an iterative process to arrive the required amount of longitudinal reinforcement. Other outcomes of the design include the stiffness and strength of the structure and the local curvature ductility demand. The versatility of the procedure is illustrated using a numerical example, which shows that reliable design results can be obtained for a wide range of structural and soil properties. The proposed procedure is relatively straightforward to implement and is deemed useful for performance-based seismic design.

**KEYWORDS:** soil-pile interaction, ductility, displacement-based design, bridge, reinforced concrete

### 1. INTRODUCTION

A cost effective design for bridge substructures involves the use of column/pile-shaft combination, often called the extended pile-shaft. The supporting column is continued below the ground level as a cast-in-drilled-hole pile, as shown in Figure 1(a), until the member reaches a depth where the vertical load bearing capacity is adequately developed. For this type of structures, the overall seismic response is characterized by an increased flexibility due to the compliance of the soil. The increased flexibility poses a special challenge in design as the large lateral displacement may lead to significant inelastic deformation in the pile-shaft with potential for unacceptable damage of the structure below ground. In order to minimize the severity of the damage in the pile-shaft, the level of the seismic displacement imposed on the structure needs to be carefully controlled. Thus, for proper design of extended pile-shafts, the influence of surrounding soil on the overall performance of the structure must be taken into account judiciously.

In this paper, a procedure for seismic design of extended pile-shafts is presented. The procedure follows the displacement-based design philosophy, where a target displacement is specified as the basis for design to ensure the satisfactory performance of the structure (Priestley *et al.* 2007). The stiffness and strength of the pile-shaft are not direct design variables but are outcomes, among other results, of the design. A secant stiffness, instead of the initial stiffness, of the pile-shaft is used to characterize the seismic response of the structure. The design procedure is developed on the basis of the analytical model presented in Song and Chai (2008). The procedure incorporates soil properties into the design process so that the influences of soil stiffness and strength on the vibrational period and lateral displacement of the structure are considered. It is shown that the design procedure is relatively straightforward to implement, but more importantly, is deemed useful for performance-based seismic design. The versatility of the procedure is illustrated using a numerical example, which shows that reliable results can be obtained for a wide range of structural and soil properties

### 2. METHODOLOGY

The proposed design procedure is suitable for multi-span bridges with individual bents supported on concrete pile-shafts that are restrained from rotation at the pile-head. The structure is assumed to have a fairly uniform distribution of strength and stiffness between bents so that seismic response of the structure may be characterized by the response of a single bridge bent modeled as a single-degree-of-freedom system under the transverse load.

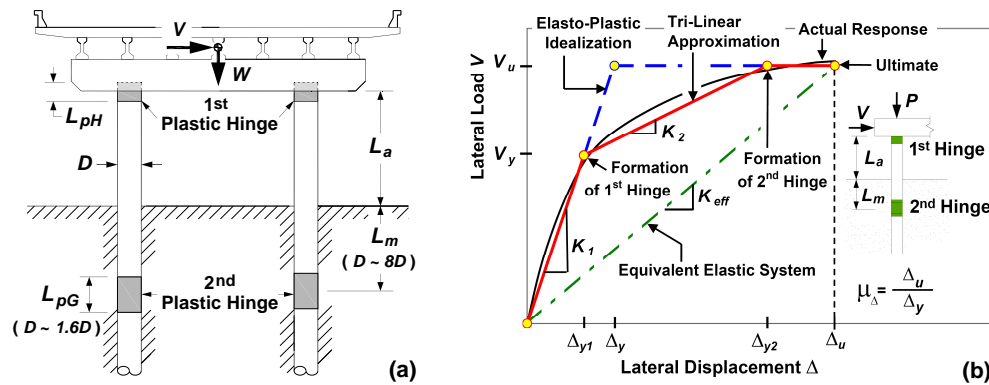


Figure 1 (a) The soil-pile system of a bridge bent supported on extended pile-shafts and (b) its lateral load-displacement relation

The bridge is assumed to be located in a high seismic risk zone so that inelastic response of the structure must be considered under the design level earthquakes. The inelastic load-displacement response of the pile-shaft can be approximated to a tri-linear curve, as shown in Figure 1(b), with the initial elastic stiffness  $K_1$ , followed by a reduced stiffness  $K_2$ , due to the development of the first plastic hinge at pile/bent-cap interface, and then by a fully plastic mechanism after the formation of the second plastic hinge below the ground level. In displacement-based design, the inelastic single-degree-of-freedom system is substituted by an equivalent elastic system having an effective stiffness  $K_{eff}$  equals to the secant stiffness, which is defined by the stiffness from the origin to the ultimate displacement  $\Delta_u$ , as also illustrated in Figure 1(b) (Priestley *et al.* 2007).

The design task at hand is to determine the amount of reinforcement for a given level of seismic demand and site condition. The design process involves nonlinear solutions and successive iterations. The following soil and structure parameters are assumed to be known at the beginning of the design process: **Structural properties:** The above-ground height  $L_a$  is known since the need to provide traffic clearance frequently dictates the above-ground height of the structure. The number of columns per bridge bent is assumed to be determined *a priori*. The seismic mass  $m$  tributary to each pile-shaft is obtained from the summation of the mass of two adjacent half spans of the superstructure and the mass of the bent-cap divided by the number of columns per bent. The material properties such as the Young's modulus  $E$  and compressive strength  $f'_c$  of concrete and the yield strength of the reinforcement  $f_y$  are also assumed to be known. **Soil properties:** In this design procedure, the soil is broadly divided into cohesive and cohesionless soils, assumed to be characterized by the undrained shear strength  $s_u$  and effective friction angle  $\phi$ , respectively. For cohesive soils, the modulus of horizontal subgrade reaction  $k_h$ , which is commonly assumed to be constant with respect to the depth, can be estimated as  $k_h = 67s_u$  (Davison 1970). For cohesionless soils, the rate of increase of modulus of horizontal subgrade reaction  $n_h$  can be estimated using the effective friction angle  $\phi$  (ATC-32 1996). It is further assumed that liquefaction will not occur at the site under the design level earthquake. Note that the undrained shear strength or friction angle affects the site response, which means the selected design spectrum must be compatible with the soil properties.

**Step 1 – Select a trial diameter  $D$ .** The trial diameter  $D$  can be selected on the basis of the aspect ratio, typically in the range of  $2 \leq L_a / D \leq 8$ . The selected diameter, however, should result in an axial stress level that is within the nominal axial stress range for reinforced concrete bridge columns, i.e.  $0.05 \leq mg / (f'_c A_g) \leq 0.15$ , where  $mg$  is the gravity compression tributary to the pile-shaft and  $A_g = \pi D^2 / 4$  is the gross sectional area.

**Step 2 – Establish the target displacement  $\Delta_u$ .** Seismic performance of a structure depends on the level of inelastic deformation that is developed locally in the critical sections, which in turn depends on the displacement or drift ratio imposed on the structure. For extended pile-shafts, a good seismic performance can be ensured conservatively by limiting the inelastic deformation of the second plastic hinge to within the limiting strain for *serviceability* so that post-earthquake repair below the ground level can be avoided. The limiting serviceability strain can be selected from the strain limits (in the plastic hinge) proposed by Priestley *et al.* (2007) for different performance limit states. In this paper, the target displacement  $\Delta_u$  is specified using the ultimate drift ratio  $\gamma_u$ , i.e.:

$$\Delta_u = \gamma_u \times (L_a + L_m) \quad (2.1)$$

where  $L_a$  is the above-ground height of the pile-shaft and  $L_m$  is the depth to the second plastic hinge. The ultimate drift ratio  $\gamma_u$ , determined using the serviceability strain limits of Priestley *et al.* (2007), is shown in Figure 2 for cohesive and cohesionless soils. It should be noted that the depth to the second plastic hinge  $L_m$  in Eqn. 2.1 depends on the ultimate strength of the pile, among other factors, and may not be accurately calculated until the design solution has converged. To start the design process, the following preliminary estimation of the depth to the second plastic hinge  $L_m$  for soil profiles  $S_E$ ,  $S_D$  and  $S_C$ , as defined by NEHRP (2001), may be used:

$$L_m^* = \frac{L_m}{D} = \begin{cases} 4.5 + 0.022(L_a^* - 19)L_a^* & \text{for NEHRP site category } S_C \\ 5.0 + 0.021(L_a^* - 20)L_a^* & \text{for NEHRP site category } S_D \\ 6.0 + 0.020(L_a^* - 22)L_a^* & \text{for NEHRP site category } S_E \end{cases} \quad (2.2)$$

where  $L_m^*$  is the normalized depth to the second hinge, and  $L_a^* = L_a/D$  is the normalized above-ground height.

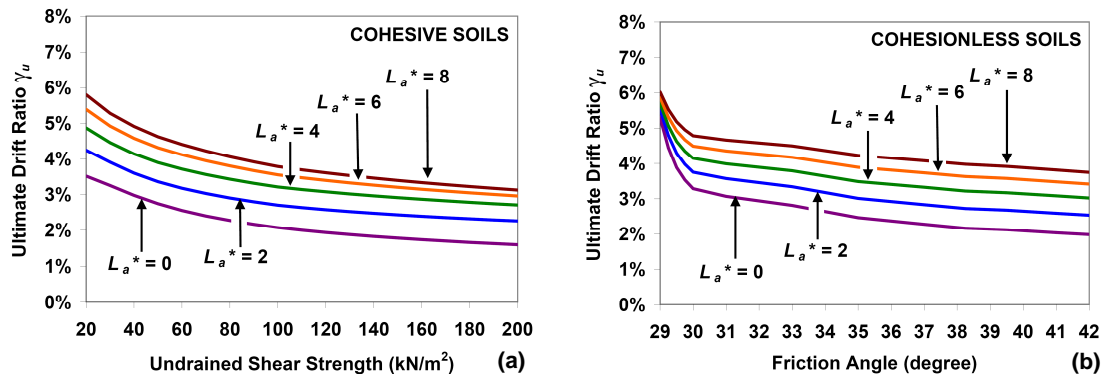


Figure 2 The ultimate drift ratio  $\gamma_u$  defined using the *serviceability* limit strain in the second plastic hinge for pile-shafts embedded in (a) cohesive soils and (b) cohesionless soils

**Step 3 – Select a displacement ductility factor  $\mu_\Delta$  and obtain the equivalent damping ratio  $\xi_{eq}$ .** As noted earlier, an iterative process is needed for the proposed displacement-based design to arrive at the required amount of longitudinal reinforcement for the pile-shaft. The process can be facilitated by iterating on the displacement ductility factor  $\mu_\Delta$  until convergence of the solution. As an initial guess, a value of  $\mu_\Delta = 3$ , corresponding to the displacement ductility limit recommended implicitly by ATC-32(1996), may be used. The design procedure then requires an estimation of the equivalent damping ratio  $\xi_{eq}$  at the displacement ductility level considered. The equivalent damping ratio is conventionally taken as the combination of the elastic damping ratio  $\xi_{el}$  and the hysteretic damping ratio  $\xi_{hyst}$  under the inelastic response. For reinforced concrete structures, the elastic damping ratio is commonly taken as  $\xi_{el} = 5\%$ . Equations relating the equivalent damping ratio to the displacement ductility factor for pile-shafts in medium sands and soft clays are available in Priestley *et al.* (2007). These equations indicate that the equivalent damping ratio increases with increasing displacement ductility factor. The rate of increase of the equivalent damping ratio reduces at large displacement ductility factors, and eventually the equivalent damping ratio tends to be at a constant level. However, a preliminary study of hysteretic damping ratio  $\xi_{hyst}$  using the experiment data of isolated extended pile-shafts by Chai and Hutchinson (2002) shows that the hysteretic damping increases linearly with increasing displacement ductility factor. Correlations between the hysteretic damping ratio and the displacement ductility factor, as extracted from the experiment results of Chai and Hutchinson (2002), are shown in Figure 3. Although the experiment result and its influence on hysteretic damping is insightful, it is nonetheless limited to only one soil type and one pile diameter and does not constitute broad enough basis for establishing the equivalent damping for the wide range of structural and soil properties expected in practice. To complete the displacement-based design procedure in this paper, equations given by Priestley *et al.* (2007) will be used, but it is recognized that refined expressions for equivalent damping ratio upon future research can be readily incorporated into the procedure.

**Step 4 – Determine the effective period  $T_{eff}$ , effective stiffness  $K_{eff}$  and lateral strength  $V_u$ .** Upon knowing the target displacement  $\Delta_u$  and the equivalent damping ratio  $\xi_{eq}$ , the effective period  $T_{eff}$  of the equivalent elastic system can be estimated using the displacement spectra for various damping ratios. The effective stiffness  $K_{eff}$  is then obtained by

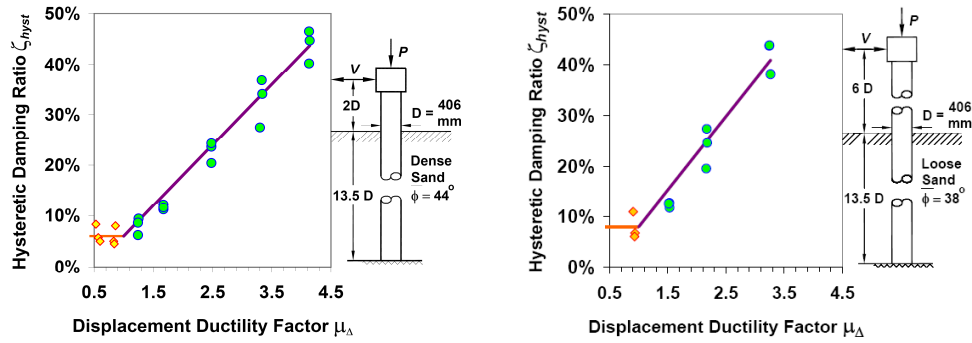


Figure 3 Correlations between the hysteretic damping ratio and the displacement ductility factor using the experiment results of Chai and Hutchinson (2002)

$$K_{eff} = \frac{4\pi^2}{T_{eff}^2} \times m \quad (2.3)$$

where  $m$  is the seismic mass per pile-shaft. The ultimate lateral strength  $V_u$  can be then determined using the equivalent elastic system shown in Figure 1(b), i.e.:

$$V_u = K_{eff} \times \Delta_u \quad (2.4)$$

**Step 5 – Determine the depth to the second plastic hinge  $L_m$  and the flexural strength  $M_u$ .** The ultimate lateral force  $V_u$  from step 4 is used to determine the depth to the second plastic hinge  $L_m$ , which is in turn related to the flexural strength of the pile and depends on the soil type, which means the depth to the second plastic hinge and the flexural strength must be evaluated separately for cohesive and cohesionless soils. For cohesive soils, the depth to the second plastic hinge, expressed in a normalized form of  $L_m^* = L_m/D$ , is given by the solution of

$$V_u^* = \begin{cases} \frac{3}{\psi_r} L_m^{*2} + 3L_m^* & \text{for } L_m^* \leq \psi_r \\ 9L_m^* - 3\psi_r & \text{for } L_m^* > \psi_r \end{cases} \quad (2.5)$$

where  $V_u^* \equiv V_u/(s_u D^2)$  is the normalized lateral strength and  $D$  is the diameter of the pile-shaft. The coefficient  $\psi_r \equiv 6s_u/(\gamma' D + 0.5s_u)$  is the critical depth coefficient for a pile embedded in cohesive soils, where  $s_u$  and  $\gamma'$  are the undrained shear strength and the effective unit weight of the soil, respectively. It is worth noting that for soft cohesive soils with small undrained shear strength, the normalized depth to the second plastic hinge will likely be greater than the critical depth coefficient, i.e.  $L_m^* > \psi_r$ . After the depth to the second plastic hinge  $L_m$  has been determined, the design flexural strength  $M_u$  can be calculated from the following equation

$$M_u = \begin{cases} \frac{s_u}{2} \left[ \frac{2L_m^3}{\psi_r} + \left( \frac{3}{2}D + 3\frac{L_a}{\psi_r} \right) L_m^2 + 3DL_a L_m \right] & \text{for } L_m^* \leq \psi_r \\ \frac{s_u}{2} \left[ \frac{9}{2}DL_m^2 + 9DL_a L_m - D^2\psi_r(3L_a + D\psi_r) \right] & \text{for } L_m^* > \psi_r \end{cases} \quad (2.6)$$

where  $L_a$  is the above-ground height of the pile-shaft. Note that the ultimate soil pressure distribution proposed by Matlock (1970) for cohesive soils has been used to determine the depth to the second plastic hinge and the design flexural strength in Eqns. 2.5 and 2.6. For cohesionless soils, the normalized depth to the second plastic hinge  $L_m^*$  and the design flexural strength  $M_u$  of the pile-shaft can be determined by

$$L_m^* = \sqrt{\frac{2}{3}V_u^*} \quad (2.7)$$

$$M_u = \frac{1}{2} \left( V_u L_a + \sqrt{\frac{8V_u^3}{27K_p\gamma'D}} \right) \quad (2.8)$$

where  $V_u^*$  is the normalized lateral strength, which is defined as  $V_u^* = V_u / (K_p \gamma' D^3)$  for cohesionless soils. The term  $\gamma'$  is the effective unit weight of the soil, and  $K_p$  is the passive soil pressure coefficient defined as  $K_p \equiv (1 + \sin \bar{\phi}) / (1 - \sin \bar{\phi})$ , where  $\bar{\phi}$  is the effective friction angle of the soil. Note that a linearly increasing ultimate soil pressure distribution proposed by Broms (1964) has been assumed in the derivation of Eqns. 2.7 and 2.8.

**Step 6 – Determine the amount of longitudinal reinforcement  $\rho_l$  and effective moment of inertia  $I_e$  of the section.** The amount of longitudinal reinforcement  $\rho_l$  for the design flexural strength  $M_u$  can readily be determined using the procedure outlined in Everard (1997). The resulting reinforcement ratio should lie in the practical range of  $0.75\% \leq \rho_l \leq 4\%$ . After calculating the longitudinal reinforcement ratio, the effective moment of inertia  $I_e$  of the pile-shaft section can be estimated. For the level of axial force currently used for design of pile-shafts, cracking of the concrete is expected to occur before the yield limit state, which would reduce the flexural rigidity of the member. The expression, proposed by Kowalsky *et al.* (1995), relating the effective moment of inertia  $I_e$  to the longitudinal reinforcement ratio  $\rho_l$  and column axial load level  $P$ , will be used:

$$I_e = \left\{ 0.21 + 12\rho_l + \left[ 0.1 + 205(0.05 - \rho_l)^2 \right] \frac{P}{f'_c A_g} \right\} I_g \quad (2.9)$$

where  $I_g = \pi D^4 / 64$  is the gross moment of inertia of the section. In estimating the effective moment of inertia, the axial force in Eqn. 2.9 may be assumed to arise entirely from the tributary weight of the superstructure, i.e.  $P = mg$ .

**Step 7 – Determine the initial elastic stiffness  $K_1$ .** The initial elastic stiffness  $K_1$  depends on the soil type and can be calculated separately using the set of equations in Table 2.1, where  $R_c$  and  $R_n$  are the characteristic length of extended pile-shaft embedded in cohesive soils and cohesionless soils, respectively.

Table 2.1 Equations for calculating the lateral stiffness of extended pile-shafts

| Parameters                      | Soil type  |  |
|---------------------------------|--|--|
|                                 | Cohesive soils   | Cohesionless soils   |
| Characteristic length           | $R_c = 4 \sqrt{\frac{EI_e}{k_h}}$ (2.10a)  | $R_n = 5 \sqrt{\frac{EI_e}{n_h}}$ (2.10b)  |
| Above-ground height coefficient | $\xi_a = \frac{L_a}{R_c}$ (2.11a)  | $\xi_a = \frac{L_a}{R_n}$ (2.11b)  |
| Initial elastic stiffness       | $K_1 = \frac{1}{\frac{1}{12} \xi_a^3 + \frac{1}{2\sqrt{2}} \xi_a^2 + \frac{1}{2} \xi_a + \frac{1}{\sqrt{2}} R_c^3} \frac{EI_e}{R_c^3}$ (2.12a) | $K_1 = \frac{1}{\frac{1}{12} \xi_a^3 + \frac{7}{16} \xi_a^2 + \frac{6}{7} \xi_a + \frac{15}{16} R_n^3} \frac{EI_e}{R_n^3}$ (2.12b) |

**Step 8 – Determine the elasto-plastic yield displacement  $\Delta_y$  and calculate the displacement ductility factor  $(\mu_\Delta)_{cal}$ .** Upon the determination of the initial stiffness  $K_1$ , the elasto-plastic yield displacement  $\Delta_y$  and displacement ductility factor  $(\mu_\Delta)_{cal}$  can be calculated using the elasto-plastic idealization shown in Figure 1(b), i.e.:

$$\Delta_y = \frac{V_u}{K_1} \quad (2.13)$$

$$(\mu_\Delta)_{cal} = \frac{\Delta_u}{\Delta_y} \quad (2.14)$$

where  $V_u$  is the ultimate lateral strength of the pile-shaft, and  $\Delta_u$  the target displacement specified in Step 2.

**Step 9 – Iterate on the displacement ductility factor until convergence.** The initial selection of the displacement ductility factor  $\mu_\Delta$  in Step 3 is unlikely to result in a converged solution in the first iteration. If the difference between the displacement ductility factor  $\mu_\Delta$  used in Step 3 and  $(\mu_\Delta)_{cal}$  given by Eqn. 2.14 is greater than a specified tolerance, say 5%, the displacement ductility factor is revised using the value from Eqn. 2.14 and the iteration returns to Step 3. The procedure cycles between Step 3 to Step 9 until the displacement ductility factor  $\mu_\Delta$  converges.

**Step 10 – Performance assessment of the pile-shaft.** Upon convergence of the solution, the lateral load-

Table 2.2 Equations defining the lateral load-displacement response of the extended pile-shafts

| Parameters   | Soil type   |   |
|--|---|---|
|  | Cohesive soils  | Cohesionless soils  |
| Lateral force at the 1 <sup>st</sup> yield limit state | $V_y = \frac{\xi_a + \sqrt{2}}{\frac{1}{2}\xi_a^2 + \sqrt{2}\xi_a + 1} \frac{M_u}{R_c} \quad (2.15a)$       | $V_y = \frac{\xi_a + \frac{7}{4}}{\frac{1}{2}\xi_a^2 + \frac{7}{4}\xi_a + \frac{13}{8}} \frac{M_u}{R_n} \quad (2.15b)$        |
| Post yield stiffness                                   | $K_2 = \frac{1}{\frac{1}{3}\xi_a^3 + \sqrt{2}\xi_a^2 + 2\xi_a + \sqrt{2}} \frac{EI_e}{R_c^3} \quad (2.16a)$ | $K_2 = \frac{1}{\frac{1}{3}\xi_a^3 + \frac{7}{4}\xi_a^2 + \frac{13}{4}\xi_a + \frac{17}{7}} \frac{EI_e}{R_n^3} \quad (2.16b)$ |

displacement response of the pile-shaft, as shown in Figure 1(b), can be generated using the analytical model presented in Song and Chai (2008). The lateral force required for the formation of the first plastic hinge  $V_y$  and the post yield stiffness  $K_2$  can be obtained using the equations given in Table 2.2. The pile-head displacement  $\Delta_{y1}$  at the first yield limit state can be calculated from  $\Delta_{y1} = V_y / K_1$ , where  $K_1$  is the initial stiffness of the soil-pile system, while the lateral displacement at the second yield limit state  $\Delta_{y2}$  can be determined from the idealized tri-linear response, i.e.:  $\Delta_{y2} = \Delta_{y1} + (V_u - V_y) / K_2$ . The curvature ductility demand  $(\mu_\phi)_{dem} = \phi_u / \phi_y$ , which signifies the level of local yielding in the pile-shaft, may be calculated by

$$(\mu_{\phi 1})_{dem} = \mu_{\phi i} - \frac{K_1}{K_2} \frac{\beta(L_m^* + L_a^*)}{\lambda_{p1}} (1 - \alpha) + \frac{\beta(L_m^* + L_a^*)}{\lambda_{p1}} (\mu_\Delta - \alpha) \quad \text{for the first plastic hinge} \quad (2.17)$$

$$(\mu_{\phi 2})_{dem} = 1 - \frac{K_1}{K_2} \frac{\beta(L_m^* + L_a^*)}{\lambda_{p2}} (1 - \alpha) + \frac{\beta(L_m^* + L_a^*)}{\lambda_{p2}} (\mu_\Delta - \alpha) \quad \text{for the second plastic hinge} \quad (2.18)$$

$$\mu_{\phi i} = 1 + \frac{K_1}{K_2} \frac{\beta(L_m^* + L_a^*)}{\eta \lambda_{p1}} (1 - \alpha) \quad (2.19)$$

where  $\lambda_{p1}$  and  $\lambda_{p2}$  are the length of the first and second plastic hinges normalized by the pile diameter  $D$ . Guidance on the estimation of the plastic hinge length for reinforced concrete pile-shafts can be found in Song and Chai (2008). The terms  $L_a^*$  and  $L_m^*$  are the normalized above-ground height and normalized depth to the second plastic hinge, respectively. The coefficient  $\alpha \equiv \Delta_{y1} / \Delta_y$  is the ratio between the displacement at the first yield limit state  $\Delta_{y1}$  and the elasto-plastic yield displacement  $\Delta_y$ . The coefficient  $\beta \equiv \Delta_y / [\phi_y (L_a + L_m)^2]$  is relating the equivalent elasto-plastic displacement  $\Delta_y$  to the elasto-plastic yield curvature  $\phi_y$  of the pile. The coefficient  $\eta$  corresponds to the ratio between the characteristic length, denoted as  $R_c$  for cohesive soils and  $R_n$  for cohesionless soils, and the distance between the two plastic hinges, i.e.  $(L_a + L_m)$  (Song and Chai 2008).

As noted previously, good seismic performance of extended pile-shaft can be ensured by limiting the inelastic deformation of the second plastic hinge to within the *serviceability* limit state. In situations where the design exceeds the recommended performance limit or a certain performance criterion cannot be satisfied by the trial diameter or target displacement, design parameters must be revised in order to arrive at a satisfactory response of the pile-shaft.

### 3. EXAMPLE

The design procedure is illustrated using a three-column bridge bent with extended pile-shafts in soft clay. The following material properties are used: (i) concrete compressive strength is  $f'_c = 34.5$  MPa and Young's modulus is  $E = 27790$  MPa, (ii) longitudinal reinforcement is provided by Grade A706 steel with yield strength of  $f_y = 414$  MPa. A concrete cover of 76 mm is assumed for the pile section. The above-ground height of the pile-shaft is  $L_a = 3.75$  m. The total mass, based on the mass of adjacent half spans of the superstructure and the mass of the bent-cap, is  $675 \times 10^3$  kg, giving a seismic mass tributary to each pile-shaft of  $m = 225 \times 10^3$  kg. The soft clay site is assumed to have an effective unit weight of  $\gamma' = 15.5$  kN/m<sup>3</sup> and an undrained shear strength of  $s_u = 40$  kN/m<sup>2</sup>, giving a modulus of horizontal subgrade reaction of  $k_h = 67 s_u = 2680$  kN/m<sup>2</sup>. Note that the soft clay site also corresponds to the soil category  $S_E$  according to NEHRP (2001). The design is conducted assuming a peak ground acceleration of  $pga = 0.4$  g. A convergence criterion of 5% is assumed for the displacement ductility factor in the design process.

**Step 1** – A trial diameter of  $D = 1.0$  m is chosen, resulting in an aspect ratio of  $L_a / D = 3.75$  for the pile-shaft. The axial stress on the pile is  $P / (f'_c A_g) = 8.1\%$ , where  $A_g = 0.79$  m<sup>2</sup>. The gross moment of inertia is  $I_g = 0.049$  m<sup>4</sup>. The critical depth coefficient of the soil-pile system is  $\psi_r = 6s_u / (\gamma D + 0.5s_u) = 6.76$ . **Step 2** – For estimating the target displacement, the ultimate drift ratio is  $\gamma_u = 4\%$  from Figure 2(a). The normalized depth to the second plastic hinge is estimated to be  $L_m^* = 4.7$  per Eqn. 2.2, giving a depth to the second plastic hinge of  $L_m = 4.7$  m. The target displacement is thus  $\Delta_u = 0.335$  m per Eqn. 2.1. **Step 3** – The iteration starts with an initial guess of the displacement ductility factor of  $\mu_\Delta = 3.0$ . Using the equation by Priestley *et al.* (2007) for fixed-head pile in cohesive soil with  $s_u = 40$  kN/m<sup>2</sup>, the equivalent damping ratio is  $\zeta_{eq} = 15\%$  for  $\mu_\Delta = 3.00$ . **Step 4** – The pile-shaft is designed with reference to a displacement design spectrum using a peak ground acceleration of  $pga = 0.4g$ , a peak ground velocity of  $pgv = 1$  m/sec and a peak ground displacement of  $pgd = 0.765$  m. The peak ground velocity and peak ground displacement have been estimated using a  $pga/pgv$  ratio of  $0.4$  g/(m/sec) and a  $(pga \times pgd)/pgv^2$  ratio of  $3$ , as guided by a study in Song *et al.* (2006) for NEHRP site category  $S_E$ . For the target displacement of  $\Delta_u = 0.335$  m and using an equivalent damping ratio of  $\zeta_{eq} = 15\%$ , the effective period of the equivalent elastic system is found to be  $T_{eff} = 1.63$  sec. The corresponding effective stiffness of the equivalent elastic system is  $K_{eff} = 3333$  kN/m from Eqn. 2.3. With  $K_{eff} = 3333$  kN/m and a target displacement of  $\Delta_u = 0.335$  m, the ultimate lateral strength of the pile-shaft is  $V_u = 1117$  kN per Eqn. 2.4. **Step 5** – Using the normalized lateral strength of  $V_u^* = V_u / (s_u D^2) = 27.93$  and the critical depth coefficient of  $\psi_r = 6.76$ , the normalized depth to the second plastic hinge obtained by solving Eqn. 2.5 is  $L_m^* = 5.24$ , giving an actual depth to the second plastic hinge of  $L_m = 5.24$  m. The substitution of  $D = 1.0$  m,  $L_a = 3.75$  m,  $L_m = 5.24$  m,  $s_u = 40$  kN/m<sup>2</sup> and  $\psi_r = 6.76$  into Eqn. 2.6 gives the design flexural strength of  $M_u = 3768$  kN-m. **Step 6** – The longitudinal reinforcement of the pile-shaft is determined using the procedure outlined by Everard (1997). The axial load  $P$  is assumed to arise entirely from the weight of the superstructure, i.e.  $P = mg = 2200$  kN. For the flexural strength of  $M_u = 3768$  kN-m, the longitudinal reinforcement ratio is found to be  $\rho_l = 2.85\%$ . The longitudinal reinforcement is assumed to be provided by uniformly distributed #32 bars. With a longitudinal reinforcement ratio of  $\rho_l = 2.85\%$ , the effective moment of inertia is  $I_e = 0.57 I_g = 0.028$  m<sup>4</sup>, as calculated using Eqn. 2.9, which gives an effective flexural rigidity of  $EI_e = 7.754 \times 10^5$  kN-m<sup>2</sup>. **Step 7** – The characteristic length from Eqn. 2.10a is  $R_c = 4.12$  m, giving an above-ground height coefficient of  $\xi_a = 0.91$  per Eqn. 2.11a. The lateral stiffness of the soil-pile system calculated from Eqn. 2.12a is  $K_1 = 7288$  kN/m. **Step 8** – For the ultimate lateral strength of  $V_u = 1117$  kN and the elastic stiffness of  $K_1 = 7288$  kN/m, the elasto-plastic yield displacement is  $\Delta_y = 0.15$  m per Eqn. 2.13. The displacement ductility factor calculated from Eqn. 2.14 is  $(\mu_\Delta)_{cal} = 2.19$ . **Step 9** – The difference between the displacement ductility factor used in Step 3, i.e.  $\mu_\Delta = 3.00$ , and the value calculated from Eqn. 2.14, i.e.  $(\mu_\Delta)_{cal} = 2.19$ , is  $27\%$ , which is much larger than the specified tolerance of  $5\%$ . In this case, the displacement ductility factor is updated using  $\mu_\Delta = 2.19$  and repeated in Step 3 until the displacement ductility factor converges. Table 3.1 shows pertinent results during the iteration. It can be seen from the table that the displacement ductility factor converges fairly rapidly, resulting in less than  $5\%$  difference after two iterations. In this case, the displacement ductility factor converges to  $\mu_\Delta = 2.15$ . The final longitudinal reinforcement ratio is  $\rho_l = 3.07\%$ , which is within the practical limits for longitudinal reinforcement.

Table 3.1 Convergence of solutions for the design of an extended pile-shaft in a NEHRP  $S_E$  cohesive soil site

| Iteration | $\mu_\Delta$ | $\zeta_{eq}$<br>(%) | $T_{eff}$<br>(sec) | $K_{eff}$<br>(kN/m) | $V_u$<br>(kN) | $L_m$<br>(m) | $M_u$<br>(kN-m) | $\rho_l$<br>(%) | $K_1$<br>(kN/m) | $\Delta_y$<br>(m) | $(\mu_\Delta)_{cal}$ | difference<br>between<br>$\mu_\Delta$ & $(\mu_\Delta)_{cal}$<br>(%) |
|-----------|--------------|---------------------|--------------------|---------------------|---------------|--------------|-----------------|-----------------|-----------------|-------------------|----------------------|---|
| 1         | 3.00         | 15.0                | 1.63               | 3333                | 1117          | 5.24         | 3768            | 2.85            | 7288            | 0.15              | 2.19                 | 27.0%   |
| 2         | 2.19         | 14.2                | 1.60               | 3459                | 1160          | 5.38         | 3963            | 3.07            | 7430            | 0.16              | 2.15                 | 1.5%  |

**Step 10** – Upon convergence, local inelastic deformations and hence a sense on the expected performance of the pile-shaft can be evaluated. The lateral force required for the formation of the first plastic hinge is  $V_y = 822$  kN, per Eqn. 2.15a. The post yield stiffness of the pile-shaft calculated by Eqn. 2.16a is  $K_2 = 2428$  kN/m. The lateral displacement at the first and second yield limit states are  $\Delta_{y1} = V_y / K_1 = 0.11$  m and  $\Delta_{y2} = \Delta_{y1} + (V_u - V_y) / K_2 = 0.25$  m, respectively. The ultimate displacement of  $\Delta_u = 0.335$  m can be converted into an ultimate drift ratio of  $\gamma_u = 3.7\%$ . The curvature ductility demand under the converged displacement ductility factor is then calculated using Eqns. 2.17 to 2.19. The dimensionless quantities  $\alpha$ ,  $\beta$  and  $\eta$  used for curvature ductility assessment are calculated as:  $\alpha = \Delta_{y1} / \Delta_y = 0.71$ ,  $\beta \equiv \Delta_y / [\phi_y (L_a + L_m)^2] = 0.38$  and  $\eta = 0.78$ . The normalized plastic hinge lengths of the first and the second plastic hinges, calculated using the guideline in Song and Chai (2008), are  $\lambda_{p1} = 0.58$  and  $\lambda_{p2} = 1.03$ , respectively. From Eqn. 2.19, the curvature ductility demand  $\mu_{\phi i}$  is  $\mu_{\phi i} = 7.80$ . The curvature ductility demands in the first and second plastic hinges, as calculated by Eqns. 2.17 and 2.18, are  $(\mu_{\phi 1})_{dem} = 11.08$  and

$(\mu_{\phi 2})_{dem} = 2.85$ , respectively. For an extended pile-shaft with a diameter of  $D = 1.0$  m and a longitudinal reinforcement ratio of  $\rho_l = 3.07\%$ , a curvature ductility capacity of  $(\mu_{\phi})_{cap} = 2.97$  is expected to be provided for the *serviceability* limit state, and the curvature ductility capacity is adequate for the curvature ductility demand of  $(\mu_{\phi 2})_{dem} = 2.85$  in the second plastic hinge. To minimize the severity of damage in the pile/bent-cap connection, the ductility limit for *damage-control* limit state should be applied to the first plastic hinge. For the selected geometry of the bridge, a confining steel ratio of  $\rho_s = 1.0\%$  is sufficient to ensure a curvature ductility capacity of  $(\mu_{\phi})_{cap} = 12.68$  for the *damage-control* limit state. The provided curvature ductility capacity is larger than the curvature ductility demand of  $(\mu_{\phi 1})_{dem} = 11.08$  in the first plastic hinge.

#### 4. CONCLUSIONS

A procedure for displacement-based seismic design of extended pile-shafts is proposed in this paper. A target displacement is specified to control the inelastic deformation in the plastic hinges of the pile-shaft so that a satisfactory seismic performance of the bridge can be ensured. The design procedure uses a secant stiffness of the soil-pile system and an equivalent damping ratio, which includes the inherent (elastic) damping and the hysteretic damping from yielding of the pile and soil. A useful feature of the procedure is that soil properties, more specifically stiffness and strength of cohesive and cohesionless soils, can be incorporated into the design process. The proposed procedure is relatively straightforward to implement, requiring relatively few design parameters: (1) above-ground height, (2) mass of the superstructure, (3) material properties, and (4) soil conditions at the bridge site. Lateral strength of the structure, local curvature ductility demands as well as the main reinforcement ratio for the pile-shaft are among the outcomes of the design procedure. Although the design process requires iteration on the displacement ductility factor, numerical example conducted in this paper shows rather rapid convergence of the design solution. Even though the procedure is illustrated using only one example, it is contended that the procedure will yield reliable design solutions and is applicable to a wide range of structural and soil properties. The versatility of the proposed procedure makes it useful for performance-based seismic design.

#### REFERENCE

- ATC-32. (1996). Improved Seismic Design Criteria for California Bridges: Provisional Recommendations, Applied Technology Council, Redwood City, California, USA.
- Broms, B.B. (1964) Lateral resistance of piles in cohesionless soils, *Journal of Soil Mechanics and Foundation Division*, ASCE, **90:3**, 123-156.
- Chai, Y.H. and Hutchinson, T.C. (2002). Flexural strength and ductility of extended pile-shafts – II: Experimental study. *Journal of Structural Engineering*, ASCE, **128:5**, 595-602.
- Davison, M.T. (1970). Lateral load capacity of piles. *Highway Research Record*, **333**, 104-112.
- Everard, N.J. (1997). Axial load-moment interaction for cross-sections having longitudinal reinforcement arranged in a circle. *ACI Structural Journal*, **94**, 695-699.
- Kowalsky, M., Priestley, M.J.N., and MacRae, G.A. (1995). Displacement-based design of RC bridge columns in seismic regions. *Earthquake Engineering and Structural Dynamics*, **24**, 1623-1643
- Matlock, H. (1970) Correlations for design of laterally loaded piles in soft clay, *Proceedings, 2nd Annual Offshore Technology Conference*, 577-594.
- National Earthquake Hazards Reduction Program (2001). NEHRP Recommended Provisions for Seismic Regulations for New Buildings and Other Structures, FEMA 368, Washington, D.C., USA.
- Priestley, M.J.N., Calvi, G.M. and Kowalsky, M. (2007). Displacement-Based Seismic Design of Structures, IUSS Press, Pavia, Italy.
- Song, S.T., Chai, Y.H. and Budek, A.M. (2006). Methodology for preliminary seismic design of extended pile-shafts for bridge structures, *Earthquake Engineering and Structural Dynamics*, **35**, 1721-1738.
- Song, S.T. and Chai, Y.H. (2008). Performance assessment of multi-column bents with extended pile-shafts under lateral earthquake loads, *The IES Journal A: Civil & Structural Engineering*, **1**, 39-54.